Available online at www.sciencedirect.com
SCIENCE DIRECT
Journal of Power Sources 146 (2005) 482–486
JOURNAL OF POWER SOURCES
www.elsevier.com/locate/jpowsour

Preparation and characterization of CoO used as anodic material of lithium battery

Jing-Shan Do *, Chien-Hsiang Weng

Department of Chemical Engineering, Tunghai University, Taichung, Taiwan 40744, Taiwan, ROC

Available online 26 April 2005

Abstract

The characteristics of CoO prepared from the calcination of $Co(OH)_2$ (precursor of CoO) in the N_2 atmosphere were analyzed, and the charge/discharge properties of CoO was also investigated in this paper. Increasing the calcination temperature from 200 to 900 °C the grain size of CoO increased from 6.59 to 31.5 nm, and the BET surface area decreased from 89.83 to 0.47 $m^2\,g^{-1}$. For CoO calcinated at 200 °C the maximum charge capacity, the coulomb efficiency and the irreversible capacity at the first cycle of Li/CoO battery were found to be 1233.57 mAh g^{-1}, 98.46% and 305.87 mAh g^{-1}, respectively. The irreversible capacity in the first cycle could be recovered in the following charge/discharge cycles.

Keywords: Cobalt oxide; Anodic material; Lithium battery; Calcination temperature

1. Introduction

The commonly used anodic material in the lithium ion battery is a carbonaceous compound due to its low cost and high operational voltage. However, the theoretical capacity of the graphite or graphitable carbons is limited to be 372 mAh g^{-1} due to the formation of LiC_6 [1]. The capacity has been much improved by the development of the highly disordered structure carbonaceous compounds prepared by the pyrolysis of organic compounds [2,3]. Recently, Co_3O_4 [4–8] and the various vanadates [9–12] have been used as the anodic materials in the lithium-ion batteries. The relative higher reversible specific capacities are obtained for Co_3O_4 and vanadates, however, the large irreversible capacity during the first cycle and the higher fading rate are found in the charge/discharge processes.

A new insertion–extraction mechanism different from the carbonaceous compounds or lithium-alloying processes is proposed by using, namely, nano-sized transition-metal oxides (MO, where M is Co, Ni, Cu or Fe) [4,6,13–21]. The reversible electrochemical reaction mechanism of the charge/discharge process for CoO was mentioned to be the decomposition of CoO to Li_2O and Co by insertion of Li^+ [13,22]. The reversible capacity of CoO is obtained to be 600–800 mAh g^{-1} in the room temperature [4,13,16]. The commercial CoO powder with particle size about 1 μm is commonly used as the anodic material in the most of the investigations. However, the electrochemical and charge/discharge characteristics of CoO used as the electroactive material of anode in the lithium-ion battery would be affected by the particle size and crystallinity of CoO. It is of interest to prepare CoO powders with different properties and be used as the anodic materials of Li-ion batteries.

In the present paper, CoO is prepared by the calcination of the precursor of $Co(OH)_2$ synthesized by the chemical precipitation under the various calcinated conditions. The characteristics of the CoO particle and the charge/discharge properties of CoO used as cathode of Li/CoO coin cell are investigated.

2. Experimental

2.1. Preparation and characterization of CoO

$Co(OH)_2$ was precipitated by mixing 100 ml of 1.0 M cobalt nitrate solution (J.T. Baker, $Co(NO_3)_2{\cdot}6H_2O$, >99.1%)

* Corresponding author. Tel.: +886 4 2359 0262; fax: +886 4 2359 0009.
E-mail address: jsdo@mail.thu.edu.tw (J.-S. Do).

0378-7753/$ – see front matter © 2005 Elsevier B.V. All rights reserved.
doi:10.1016/j.jpowsour.2005.03.095

and 500 ml of 0.4 M sodium hydroxide solution (Merck, NaOH, >99%) in a flask and stirring for 8 h under 99.995% nitrogen atmosphere. The obtaining $Co(OH)_2$ was dried in a vacuum oven at 50 °C for 24 h. Cobalt oxides were obtained by the calcination of $Co(OH)_2$ in a oven with various conditions.

The crystallographic information, surface area, surface morphologies and particle size of the preparing CoO were analyzed by X-ray powder diffraction (XRD, Shimadzu XRD-6000), BET surface analyzer (Micrometritics 2375) and SEM (Joel JSM-5400), respectively.

2.2. Cells assembling and measurements

The cobalt oxide electrodes were made by scraping and pressing the paste, which was prepared by dispersing the suitable compositions of the carbon black, PVDF (poly(vinylidene fluoride)) and the preparing CoO powder with NMP (*N*-methyl-2-pyrrolidinone) as solvent, on the Cu foil. The thickness and the loading of CoO were measured to be 80–100 μm and 5.5–7.0 mg, respectively. The electrolyte, separator and counter electrode of the coin cell were 1.0 M $LiPF_6$ EC–DEC (ethylene carbonate–diethyl carbonate, provided by FERRO) (v/v 1:1), PP (polypropylene) film (Ashahi N910) and Li foil, respectively. The cells were assembled in an argon-filled glove-box (VAC MO-5). The coin cells were galvanostatically charged and discharged at a suitable C-rate, and the voltage behavior against the time was recorded over the potential range of 0.02–3.0 V (versus Li/Li^+). The coin cell was first discharged from the open circuit voltage (OCV) to 0.02 V, and then charged and discharged between 0.02 and 3.0 V in the following cycles.

3. Results and discussion

3.1. Characteristics of $Co(OH)_2$ and CoO

The main product of the precipitation by mixing the $Co(NO_3)_2$ and NaOH aqueous solutions with aging period greater than 1 h was the brucite-like compound with the formula $Co^{II}(OH)_2{\cdot}0.03H_2O$ [23]. Comparing the XRD pattern of $Co(OH)_2$ precipitate with the patterns in the literatures [23,24] revealed that the preparing $Co(OH)_2$ was the brucite-like formula. A slice-like structure with the particle size of 200 nm was found in the SEM photograph of $Co(OH)_2$, and the grain size of $Co(OH)_2$ obtained from the XRD analysis was 22.9 nm (Table 1).

CoO can be obtained by the decomposition of $Co(OH)_2$ in an elevated temperature. For the presence of a trace of oxygen in the furnace CoO can be further oxidized to Co_3O_4. The pure phase of CoO was obtained for $Co(OH)_2$ calcinated in a tubular furnace at 99.995% N_2 atmosphere (Fig. 1). The XRD patterns exhibited the characteristic peaks of CoO at 36.5°, 42.4°, 61.5°, 73.7° and 77.6°, and as the temperature increased, the intensities of peaks increased. The results indicated that the crystallinity of CoO increased with the calcination temperature. The average grain size was calculated based on the Sherrer equation [25] at $2\theta = 42.4°$. Increasing the calcination temperature from 200 to 300 °C the grain size changed slightly from 6.59 to 6.77 nm, and the surface area was slightly decreased from 89.82 to 68.04 $m^2\ g^{-1}$ as shown in Table 1. The grain size of CoO calcinated at 200 and 300 °C was significantly less than that of the precursor $Co(OH)_2$, indicating that the $Co(OH)_2$ crystallite was cracked at the calcination process due to the decomposition of $Co(OH)_2$ to CoO and loss of H_2O. Furthermore the slice structure similar to the precursor $Co(OH)_2$ was found for CoO prepared at 200 and 300 °C. The surface area of CoO prepared at 200 and 300 °C was hence greater than its precursor (Table 1).

Table 1
Effect of calcination temperature on the grain size and the BET surface area of CoO

T (°C)	Grain size (nm)	BET surface area ($m^2\ g^{-1}$)
–[a]	22.9	28.05
200	6.59	89.83
300	6.77	68.04
400	14.2	36.81
500	26.3	16.49
600	27.3	9.18
700	28.4	4.32
800	30.9	1.07
900	31.5	0.47

Calcination time = 1 h; 99.995% N_2 atmosphere.
[a] Precursor of CoO.

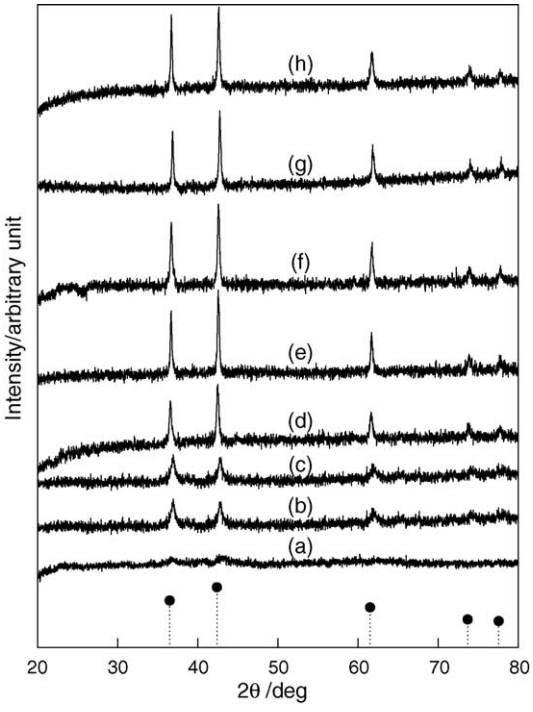

Fig. 1. XRD patterns of cobalt oxide calcinated in tubular furnace, $t = 1$ h, 99.995% N_2 atmosphere. Calcination temperatures: (a) 200 °C, (b) 300 °C, (c) 400 °C, (d) 500 °C, (e) 600 °C, (f) 700 °C, (g) 800 °C and (h) 900 °C.

Increasing the temperature from 400 to 900 °C the crystallinity and the particle size of CoO significantly increased as shown in the XRD patterns (curves (c)–(h) of Fig. 1) and the SEM analysis, resulting in the increase of the grain size of CoO from 14.2 to 31.5 nm and the decrease of the surface area from 36.81 to 0.47 $m^2\ g^{-1}$.

3.2. Charge/discharge properties of CoO electrode contained 10% carbon black

The charge/discharge rate (C-rate) of Li/CoO coin cell was calculated based on the theoretical discharge capacity of the electroactive material CoO. The theoretical discharge capacity of CoO was based on the following charge/discharge process to be 715.4 mAh g^{-1} [13]

$$CoO + 2Li^+ + 2e^- \rightleftharpoons Li_2O + Co \quad (1)$$

The utility of the electroactive material CoO would be restricted by its low electric conductivity. The addition of carbon black used as the conducting agent could promote the conductivity of the electrode and the utility of the electroactive material. Using CoO calcinated at 600 °C as electroactive material, the weight fractions of CoO, carbon black and PVDF in the electrode were 0.80, 0.10 and 0.10, respectively. The charge/discharge curves of the CoO electrode with 0.1 C-rate were given in Fig. 2. The results indicated that the discharge voltage decreased sharply from the OCV to the discharge plateau of 0.8 V. The discharge plateau voltage increased to 1.0–1.5 V in the second cycle. The grain size of CoO calcinated at 600 °C was found to be 27.3 nm (Table 1). CoO was decomposed to Co and Li_2O with the grain size of 1–2 nm in the first discharge cycle [13]. Therefore the grain size of CoO formed in the first charge process (back reaction of (1)) would be same as the grain size of Co or Li_2O formed in the first discharge cycle, i.e. 1–2 nm. The change in the voltage of discharge plateau in the first and second cycles was hence caused by the significant change in the grain size of CoO.

Increasing the discharge cycle number from 2 to 39 the voltage of discharge plateau decreased from 1.0–1.5 to 0.8–1.2 V (Fig. 2). The experimental results might be due to the increase of the internal resistance of CoO electrode in the charge/discharge process. The discharge capacity in the voltage range of 0.8–0.02 V in Fig. 2 was inferred as the formation of polymer/gel-like film [17,18,20,21]. This polymer/gel-like film was reversible and disappeared in the following charge process (Fig. 2).

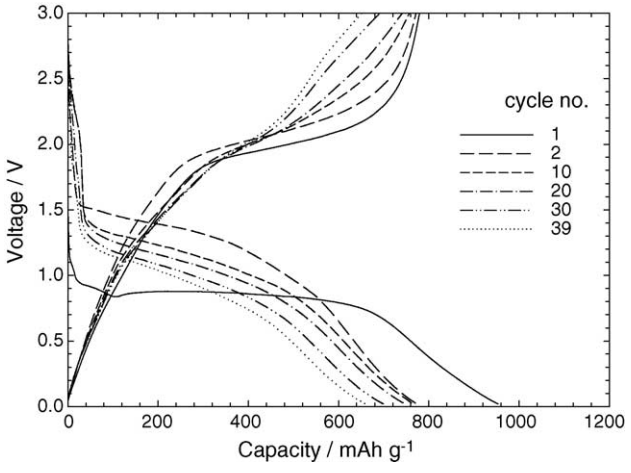

Fig. 2. Charge/discharge curves of Li/CoO (calcinated at 600 °C, 10% carbon black) coin cell. Weight fractions of CoO electrode: CoO(0.8), carbon black(0.1), PVDF(0.1), anode: Li foil, electrolyte: 1.0 M $LiPF_6$ EC–DEC (v/v 1:1) solution, room temperature, potential range of charge/discharge: OCV ~0.02 V (first discharge cycle), 3.0–0.02 V (others), cycling rate = 0.1 C.

3.3. Effect of the CoO calcination temperature

As described in the above, the decrease of the discharge capacity for the cycle number greater than 2 was deduced to be the increase of the internal resistance of CoO electrode in the presence of 10% carbon black. Hence the weight fraction of carbon black in the CoO electrode was increased to 20% to reduce the internal resistance. In the presence of 20% carbon black the discharge capacity of CoO electrode increased with the cycle number (activation period) was found for CoO prepared with various temperatures (Fig. 3). In general, the cycle number of activation period increased with the CoO preparing temperature.

The activation period was deduced as the cycle number for recovery of the irreversible capacity, which was caused by some of the irreversible Li_2O generated in the first discharge

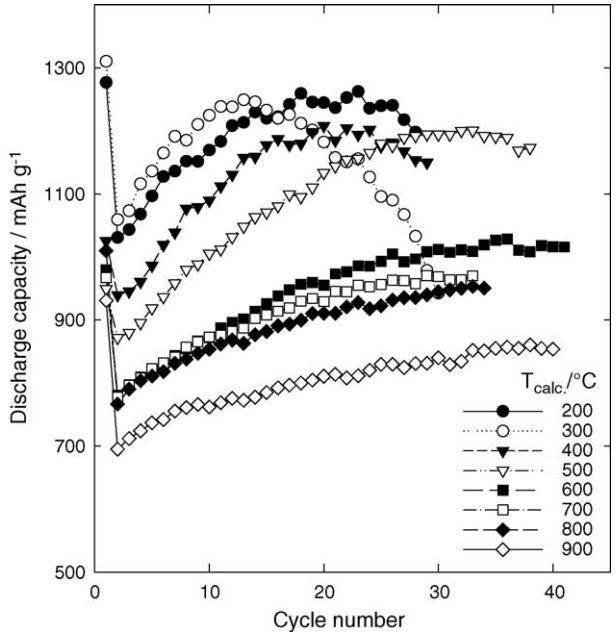

Fig. 3. Effect of cycle number on the discharge capacity of Li/CoO coin cell. Weight fractions of CoO electrode: CoO(0.6), carbon black(0.2), PVDF(0.2), anode: Li foil, electrolyte: 1.0 M $LiPF_6$ EC–DEC (v/v 1:1) solution, room temperature, potential range of charge/discharge: OCV ~0.02 V (first discharge cycle), 3.0–0.02 V (others), cycling rate = 0.1 C.

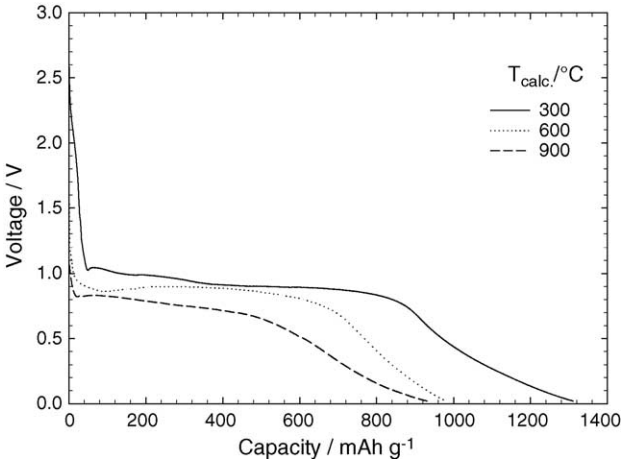

Fig. 4. Discharge curves of Li/Co coin cell. Weight fractions of CoO electrode: CoO(0.6), carbon black(0.2), PVDF(0.2), anode: Li foil, electrolyte: 1.0 M $LiPF_6$ EC–DEC (v/v 1:1) solution, room temperature, potential range of charge/discharge: OCV ~0.02 V (first discharge cycle), 3.0–0.02 V (others), cycling rate = 0.1 C.

cycle. In the presence of sufficient carbon black (20%) the configuration of CoO electrode rearranged and the contact of components in the electrode increased with the cycle number. The irreversible Li_2O formed in the first discharge cycle was gradually reacted back to CoO and Li^+. Decreasing the CoO calcination temperature decreased the particle size of CoO, and increased the uniformity of the electrode compositions after the first discharge process. Therefore the period (cycle number) for rearranging the electrode compositions and obtaining an optimal contact of the compositions to recover the irreversible discharge capacity decreased with the decrease of CoO calcination temperature.

As shown in Fig. 4, the discharge plateau of CoO electrode in the first cycle were found to be 1.05–0.80, 0.90–0.73 and 0.80–0.50 V, respectively, when CoO was prepared at the calcination temperature of 300, 600 and 900 °C. The higher the plateau voltage in the first discharge process revealed that the reaction of CoO with Li^+ to be Co and Li_2O was more readily. It was mainly caused by the decrease of the grain size of CoO with the decrease of the calcinated temperature.

The experimental results indicated that the discharge capacity in the first cycle increased from 930.8 to 1310.5 mAh g^{-1} with the decrease of the CoO calcination temperature from 900 to 300 °C (Fig. 3). The results in Fig. 4 also revealed that both of the capacity caused by the reaction (1) (discharge plateau) and the formation of polymer/gel-like substances increased with the decrease of calcination temperature. Decreasing the grain and particle sizes of CoO increased the contact of CoO and the conducting agent, and the utility of the electroactive material in the electrode increased. Hence the discharge capacity due to the reaction (1) increased from 620 to 840 mAh g^{-1} with the decrease of the CoO calcination temperature from 900 to 300 °C. The formation of polymer/gel-like substances was also promoted with a smaller grain size of CoO.

Although the discharge capacity of CoO increased with the decrease of the CoO clacination temperature, CoO prepared at a higher temperature had a lower rate of discharge capacity fading (Fig. 3).

4. Conclusions

The brucite-like compound of $Co(OH)_2{\cdot}0.03H_2O$ obtained by the chemical precipitation was calcinated in a tubular furnace in the presence of high purity N_2 at 200–900 °C to prepare CoO. Increasing the CoO calcination temperature from 200 to 900 °C increased the grain size from 6.59 to 31.5 nm, and decreased the surface area from 89.82 to 0.47 $m^2\ g^{-1}$. The irreversible discharge capacity due to the loss of contact of CoO with the conducting agent could be recovered in the following charge/discharge cycles due to the reconfiguration of the structure of CoO electrode in the presence of 20% carbon black. The activation cycles for the recovery of the irreversible discharge capacity decreased with the decrease in the CoO calcinated temperature. The discharge capacity in the first cycle and the maximum discharge capacity other than first cycle increased from 930.8 and 854.9 to 1276.9 and 1244.8 mAh g^{-1}, respectively, when the CoO calcination temperature decreased from 900 to 200 °C.

Acknowledgments

The financial support of Ministry of Education of Republic of China (Project number: EX-91-E-FA09-5-4) and Tunghai University is acknowledged.

References

[1] B. Scrosati, Electrochim. Acta 45 (2000) 2461.
[2] K. Sato, M. Noguchi, A. Demachi, N. Oki, M. Endo, Science 264 (1994) 556.
[3] J.R. Dahn, T. Zheng, Y. Liu, J.S. Xue, Science 270 (1995) 590.
[4] F. Badway, I. Plitz, S. Grugeon, S. Laruelle, M. Dollé, A.S. Gozdz, J.-M. Tarascon, Electrochem. Solid State Lett. 5 (2002) A115.
[5] G.X. Wang, Y. Chen, K. Konstantinov, J. Yao, J. Shn, H.K. Liu, S.X. Dou, J. Alloys Comp. 340 (2002) L5.
[6] G.X. Wang, Y. Chen, K. Konstantinov, M. Lindsay, H.K. Liu, S.X. Dou, J. Power Sources 109 (2002) 142.
[7] D. Larcher, G. Sudant, J.-B. Leriche, Y. Chabre, J.-M. Tarascon, J. Electrochem. Soc. 149 (2002) A234.
[8] Y.-M. Kang, K.-T. Kim, K.-Y. Lee, S.-J. Lee, J.-H. Jung, J.-Y. Lee, J. Electrochem. Soc. 150 (2003) A1538.
[9] S. Denis, E. Baudrin, M. Touboul, J.-M. Tarascon, J. Electrochem. Soc. 144 (1997) 4099.
[10] E. Baudrin, S. Laruelle, S. Denis, M. Touboul, J.-M. Tarascon, Solid State Ionics 123 (1999) 139.
[11] S. Denis, E. Baudrin, F. Orsini, G. Ouvrard, M. Touboul, J.-M. Tarascon, J. Power Sources 81–82 (1999) 79.
[12] S. Laruelle, P. Poizot, E. Baudrin, V. Briois, M. Touboul, J.-M. Tarascon, J. Power Sources 97–98 (2001) 251.
[13] P. Poizot, S. Laruelle, S. Grugeon, L. Dupont, J.-M. Tarascon, Nature 407 (2000) 496.
[14] J.-M. Tarascon, M. Armand, Nature 414 (2001) 359.

[15] S. Grugeon, S. Laruelle, R. Herrera-Urbina, L. Dupont, P. Poizot, J.-M. Tarascon, J. Electrochem. Soc. 148 (2001) A285.
[16] S. Grugeon, S. Laruelle, P. Poizot, J.-M. Tarascon, US Patent WO 200,171,833 (2001).
[17] S. Laruelle, S. Grugeon, P. Poizot, M. Dollé, L. Dupont, J.-M. Tarascon, J. Electrochem. Soc. 149 (2002) A627.
[18] M. Dollé, P. Poizot, L. Dupont, J.-M. Tarascon, Electrochem. Solid State Lett. 5 (2002) A18.
[19] M. Morcrette, F. Gillot, L. Monconduit, J.-M. Tarascon, Electrochem. Solid State Lett. 6 (2003) A59.
[20] S. Grugeon, S. Laruelle, L. Dupont, J.M. Tarascon, Solid State Sci. 5 (2003) 895.
[21] R. Dedryvere, S. Laruelle, S. Grugeon, P. Poizot, D. Gonbeau, J.-M. Tarascon, Chem. Mater. 16 (2004) 1056.
[22] H.C. Choi, S.Y. Lee, S.B. Kim, M.G. Kim, M.K. Lee, H.J. Shin, J.S. Lee, J. Phys. Chem. B 106 (2002) 9252.
[23] Z.P. Xu, H.C. Zeng, J. Mater. Chem. 8 (1998) 2499.
[24] Z.P. Xu, H.C. Zeng, Chem. Mater. 11 (1999) 67.
[25] C. Lin, J.A. Ritter, B.N. Popov, J. Electrochem. Soc. 145 (1998) 4097.